the FEBS Journal

Interaction with model membranes and pore formation by human stefin B – studying the native and prefibrillar states

Sabina Rabzelj[1,*,†], Gabriella Viero[2,*,‡], Ion Gutiérrez-Aguirre[3], Vito Turk[1], Mauro Dalla Serra[2], Gregor Anderluh[3] and Eva Žerovnik[1]

1 Department of Biochemistry and Molecular Biology, Jožef Stefan Institute, Ljubljana, Slovenia
2 Fondazione Bruno Kessler and CNR-Istituto di Biofisica, Povo, Trento, Italy
3 Department of Biology, Biotechnical Faculty, University of Ljubljana, Slovenia

Keywords
amyloid pores; amyloid–lipid interaction; cystatin C; EPM1 mutants; surface plasmon resonance

Correspondence
G. Anderluh, Department of Biology, Biotechnical Faculty, University of Ljubljana, Večna pot 111, 1000 Ljubljana, Slovenia
Fax: +386 1 257 33 90
Tel: +386 1 423 33 88
E-mail: gregor.anderluh@bf.uni-lj.si
E. Žerovnik, Department of Biochemistry and Molecular Biology, Jožef Stefan Institute, Jamova 39, 1000 Ljubljana, Slovenia
Fax: +386 1 477 39 84
Tel: +386 1 477 3753
E-mail: eva.zerovnik@ijs.si

Present address
†Bia d.o.o., Ljubljana, Slovenia
‡Laboratory of Translational Genomics, CIBIO - Center for Integrative Biology, Mattarello, Trento, Italy

*These two authors contributed equally to this work

(Received 25 January 2008, revised 25 February 2008, accepted 10 March 2008)

doi:10.1111/j.1742-4658.2008.06390.x

Human stefin B, from the family of cystatins, is used as a model amyloidogenic protein in studies of the mechanism of amyloid fibril formation and related cytotoxicity. Interaction of the protein's prefibrillar oligomers/aggregates with predominantly acidic phospholipid membranes is known to correlate with cellular toxicity. In the present study, we measured membrane interaction of the prefibrillar and native states for three variants: the Y31 isoform studied previously, the wild-type protein and the G4R mutant; the latter is observed in progressive myoclonus epilepsy of type 1. In addition to using critical pressure and surface plasmon resonance, we assessed membrane permeabilization by calcein release and electrophysiological measurements. It was demonstrated for the first time that wild-type stefin B and the Y31 isoform are able to form pores in planar lipid bilayers, whereas G4R destroys the bilayer by a non pore-forming process. Similarities to other amyloidogenic proteins and the possible physiological implications of our findings are discussed.

Aberrant protein folding and amyloid fibril formation is a common feature of many conformational diseases (i.e. systemic amyloidoses, such as diabetes type II, and neurodegenerative diseases, including Alzheimers's, Parkinson's, motor neuron disease and prion diseases) [1]. The accumulating evidence suggests that protein folding to an alternative conformation, forming oligomeric structures, might be an initial trigger of

Abbreviations
EPM1, myoclonus epilepsy of type 1; LUV, large unilamelar vesicles; PC, phosphatidylcholine (1,2-dioleoyl-*sn*-glycero-3-phosphocholine); PG, phosphatidylglycerol (1-palmitoyl-2-oleoyl-*sn*-glycero-3-[phospho-*rac*-(1-glycerol)]); PLM, planar lipid membrane; PS, phosphatidylserine [1,2-dioleoyl-sn-glycero-3-(phospho-L-serine)]; SPR, surface plasmon resonance.

the disease [1,2], followed by other consequences, such as Ca^{2+} and metal ions imbalance, oxidative stress, and chaperone and ubiquitin proteasome systems overload [3]. It has been proposed that amyloid fibril formation is a generic property of proteins [2,4]. This may be true also for cellular toxicity because even the prefibrillar aggregates of proteins not linked to disease were found to be toxic [5,6]. A generic mechanism for toxicity of pathological or nonpathological amyloidogenic proteins was further suggested when an antibody directed to a common structural epitope of the prefibrillar oligomers was produced [7]. In most cases, amyloid fibril formation is a stepwise mechanism involving various prefibrillar species: from globular and annular oligomers to chain-like protofibrils [8]. Research is still ongoing as to whether the oligomers are an on- or off-pathway in the amyloid fibrillation reaction [9].

At culprit for toxicity are globular oligomers of a certain size [8], which may exert toxicity by interaction with cellular lipid membranes [10,11]. The challenging 'channel hypothesis' of Alzheimer's disease [12] states that cytotoxicity is a consequence of cellular membrane permeation by prefibrillar aggregates [12–14]. Amyloidogenic proteins or peptides can form ion channels within planar lipid bilayers and cause the influx of Ca^{2+} ions, which finally leads to cell death [13]. The deleterious effect of the prefibrillar oligomers is assumed to be mediated either by means of membrane poration [8,15] or, most likely, by specific ionic transport through ion channels [16,17]. Amyloidogenic proteins form morphologically compatible ion-channel-like structures and elicit single ion-channel currents [18]. Some studies [19] prefer the term pores to emphasize the fact that 'amyloid channels' are often heterogenous and rather nonspecific. It should be noted that certain membrane micro-domains, the so-called lipid rafts, have been identified as the sites where amyloid oligomers concentrate and undergo conformational change. The process is influenced by direct binding to different gangliosides and by cholesterol content [20,21].

Stefin B belongs to the family of cystatins, which are cysteine proteases inhibitors [22]. Human cystatin C is a well known amyloidogenic protein, causing hereditary cystatin C amyloid angiopathy [23] due to the mutation L68Q. It is implied in Alzheimer's disease where its polymorphism may present a risk factor [24]. It was found to co-aggregate with Aβ in senile plaques [25] and to interfere with Aβ fibrillogenesis *in vitro* [26]. Other cystatins, also including stefins A and B, were found to co-deposite in plaques of various origin [27]. Stefin B does not cause amyloid pathology. Its main pathology remains the syndrome of progressive myoclonus epilepsy of type 1 (EPM1) [28]. However, based on *in vitro* properties, we proposed that at least some of the EPM1 mutants could aggregate in the cell and cause some of the EPM1 symptoms, such as increased oxidative stress and neurodegenerative changes [29].

We have used stefin B as a suitable amyloidogenic protein model. We have previously determined the conditions where it undergoes amyloid fibril formation and studied the mechanism of fibrillation [30,31]. Stefin B undergoes amyloid fibril formation already at pH 4.8 *in vitro* [30,31]. The reaction starts with an extensive lag phase where granular prefibrillar aggregates, composed of a range of oligomers, accumulate. In a previous study, we studied the interaction of the prefibrillar state of stefin B with phospholipid mono- and bilayers [11]. Prefibrillar states were induced by lowering the pH to 4.8 or 3.3, where the protein is initially in a native-like or molten globule state, respectively. Both states were able to bind to the membranes and were more toxic than the native state [11]. In the present study, we compare the behaviour of the Y31 isoform of stefin B studied previously, wild-type stefin B and a mutant G4R of the wild-type. The G4R mutant of the wild-type was observed in some patients with the EPM1 syndrome. Using a range of biophysical approaches, we show that negatively charged membranes are indeed better substrates for all the stefin variants in the prefibrillar state and that the EPM1 mutant G4R undergoes much stronger association with the membranes than the other two proteins. A new contribution of the present study is the finding that the wild-type stefin B and a nonpathological variant of stefin B are able to induce pores in planar lipid membranes (PLMs). Interestingly, even the wild-type protein in the native state is able to form pores with defined electrophysiolgical properties. The results obtained show that prefibrillar forms of human stefin B exhibit pore-forming characteristics similar to some other amyloidogenic proteins and peptides.

Results

In the present study, we compared the membrane interaction and pore formation properties of native and prefibrillar forms of three stefin B variants. We used a range of biophysical approaches to identify stefin B–membrane interactions and to show how these interactions are affected by the composition of the lipid membranes. The following phospholipids were used: 1,2-dioleoyl-*sn*-glycero-3-phosphocholine (phosphatidylcholine, PC), a basic building block of the cellular membranes, and negatively charged lipids

1-palmitoyl-2-oleoyl-*sn*-glycero-3- [phospho-*rac*-(1-glycerol)] (phosphatidylglycerol, PG) or 1,2-dioleoyl-sn-glycero-3-(phospho-L-serine) (phosphatidylserine, PS), which are predominately found in lipid membranes within the cell (i.e. phospatidylserine in the inner leaflet of the plasma membrane and phosphatidylglycerol in the inner mitochondrial membrane).

Insertion into lipid monolayers

We have followed the kinetics of the surface pressure increase due to protein insertion into lipid monolayers and determined the final increment in the surface pressure, which was plotted against the applied initial pressures to generate critical pressure plots (Fig. 1). The critical pressure (π_c) is the initial pressure under which no protein can insert in the monolayer. Insertion of native and prefibrillar StB-wt in PC or PG monolayers was low, aberrant and distinctly different from insertion curves of the other two variants (data not shown). This may indicate that the native state undergoes a slow conformational change on the membrane surface. Lipid membranes themselves may modulate fibrillation because some peptides and proteins aggregate more strongly on a membrane surface [32]. The highest critical pressures (Fig. 1 and Table 1) of approximately 27 $mN{\cdot}m^{-1}$ were observed for the G4R prefibrillar aggregates in both PC and PG monolayers and for the StB-Y31 prefibrillar aggregates in PG monolayers. Critical pressure of the StB-wt native state was distinctly lower (13.4 $mN{\cdot}m^{-1}$ in PC and 16.8 $mN{\cdot}m^{-1}$ in PG monolayers), whereas it raised to approximately 25 $mN{\cdot}m^{-1}$ for the prefibrillar state and both types of membranes (Table 1), in a similar way to the other two variants. However, the slope of the curves in Figs 1B,D are distinctively different for the StB-wt and other two variants, indicating that the mode of interaction with the monolayer is different in each case.

Permeabilization of large unilamelar vesicles (LUV)

We measured calcein release after incubation of stefin variants with calcein-loaded LUV. The permeabilization of PC LUV was negligible in all cases, whereas negatively charged vesicles were more susceptible (Fig. 2). The permeabilization was protein concentration dependent (Fig. 2A). After the overnight incubation of prefibrillar aggregates or native states with LUV, the highest permeability was obtained with the G4R mutant, more than 70% in both states, followed by StB-Y31. In all cases, permeabilization of StB-wt was below 10%.

Surface plasmon resonance (SPR) measurements

We studied the binding of stefin B variants by using supported liposomes in a SPR assay. We immobilized PC or PG LUV on the surface of a Biacore L1 chip (GE Healthcare, Biacore, Uppsala, Sweden) and measured the binding of stefin B variants, which were flown across the surface of the chip. Proteins were injected for 2 min at a concentration in the range 10–70 μM and allowed to dissociate for 5 min. The

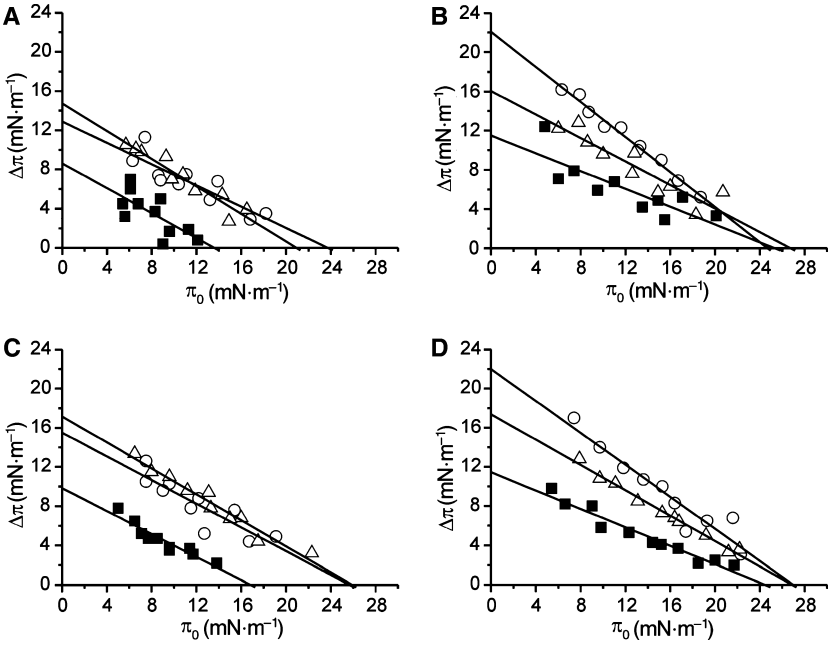

Fig. 1. Critical pressure plots. Data are for lipid monolayers of PC (A, B) and PG (C, D). Data are for the native proteins in (A, C) and for the prefibrillar form of proteins in (B, D). ■, StB-wt; ○, StB-Y31; △, G4R.

Table 1. Critical pressures for the insertion of stefin B variants into lipid monolayers. Critical pressures were determined from intersections of linear fit of the data with *x*-axis of plots presented in Fig. 1.

	π_c (mN·m^{-1})	
Protein	PC	PG
Native		
StB-wt	13.4	16.8
StB-Y31	23.7	25.7
G4R	20.9	25.9
Prefibrillar		
StB-wt	25.3	24.5
StB-Y31	24.7	27.0
G4R	26.7	26.9

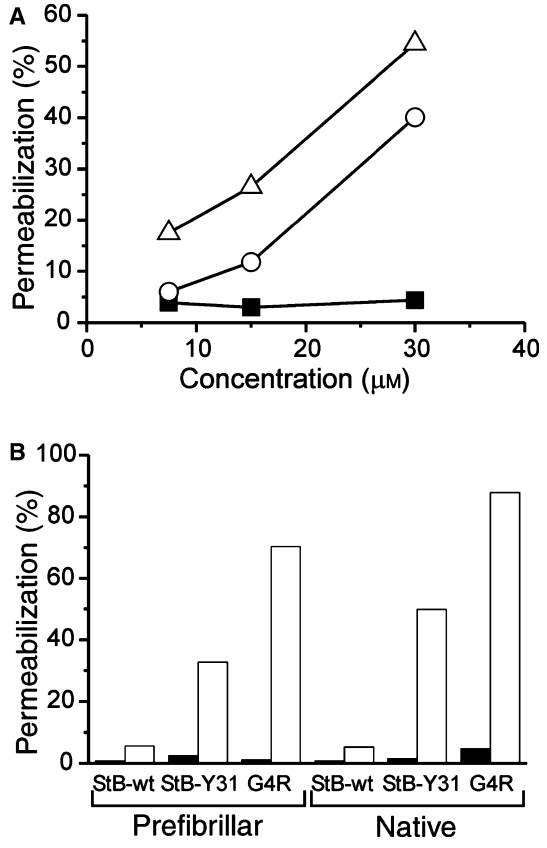

Fig. 2. Calcein release experiments. (A) The concentration dependence of calcein release of PG LUV. Liposomes were incubated for 30 min with proteins at pH 7.3. ■, StB-wt; ○, StB-Y31; △, G4R. (B) Permeabilization of calcein-loaded LUV induced by stefin variants after overnight incubation at room temperature. The concentration of proteins was 30 μM. Black columns, LUV composed of PC; white columns, LUV composed of PG. The results presented in both panels are the average of two independent experiments. The concentration of lipids was 30 μM in both panels. Each measurement was repeated at least twice.

StB-wt and G4R did not bind considerably to PC liposomes at any pH, whereas StB-Y31 bound strongly, with almost no dissociation (Fig. 3A). No variant bound to PG LUV at any extent when applied in its native state at pH 7.3 (Fig. 3B–D, thick lines), whereas the prefibrillar states at pH 4.8 bound extensively (Fig. 3B–D). The binding of the prefibrillar forms was concentration dependent in all cases (Fig. 3B–D). At the same concentration of the prefibrillar aggregates, G4R bound stronger than the tyrosine 31 isoform and, again, this was stronger that the wild-type protein. The dissociation of the G4R and StB-wt was fast and almost complete within 5 min, whereas the dissociation of StB-Y31 was slower and a considerable amount of the protein remained attached to the membranes.

Planar lipid membrane (PLM) experiments

The ability of stefin B variants to spontaneously incorporate into model membranes and to form pores was tested on PLM. PLM were prepared from the mixture of lipids that contains negatively charged PS (PC : PS, 2 : 1) because the interaction of proteins was best in negatively charged membranes (see above). The native StB-wt inserts into PLM comprised of negatively charged lipids (Fig. 4). The interaction of the protein with the lipid bilayer perturbs membrane permeability when applying either negative or positive voltages. StB-wt causes step-like increases in the current (Fig. 4A,B). Pore forming activity of the wild-type was observed a few seconds after protein addition and exhibited multiple conductance states (Fig. 4C). In both KCl and NaCl salt buffers, pore conductances are very similar (Table 2). The higher conductance state at +40 mV (level 3 in Fig. 4A,C) has a value of 512 ± 95 pS or 453 ± 22 pS in KCl or NaCl, respectively. High conductance pores were found to be stable (i.e. once they have been inserted, they remain open) (Fig. 4A). Two lower conductance states could also be observed in addition to the stable pores. They are less stable (levels 1 and 2 in Fig. 4A) and are characterized by fast opening and closing. Moreover, the pore formation process and the presence of different conductance levels did not directly depend on the applied voltage, similar to that observed for some other amyloid peptides [33,34]. StB-wt in the prefibrillar state only increased the capacitance of the membrane, without any pore formation. This effect has been recently observed for other amyloid oligomers, suggesting that these proteins could also act by thinning the membrane [30].

StB-Y31 variant in native and prefibrillar form inserts into the PLM comprised of negatively charged

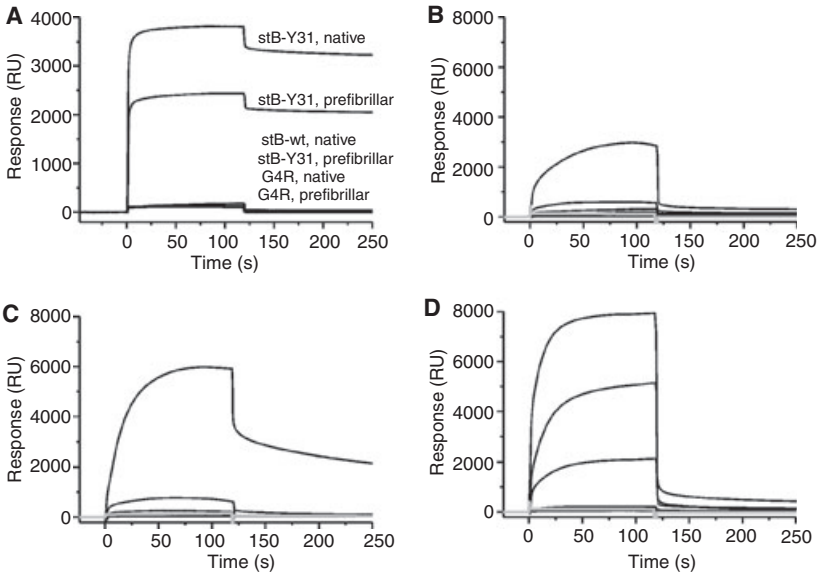

Fig. 3. Binding to liposomes measured by SPR. (A) Binding to PC LUV. A comparison of binding of 70 μM stefin variants to PC LUV immobilized on the surface of a L1 sensor chip. (B–D) A comparison of the binding of prefibrillar form of stefin variants to PG LUV. The concentration of the protein was 10, 20, 40, 50, 60 and 70 μM (curves from the bottom to the top) in each case. The thick gray line represents binding of native stefin variants at 70 μM. (B) StB-wt; (C) StB-Y31; (D) G4R. The curves are representative examples of at least two independent experiments.

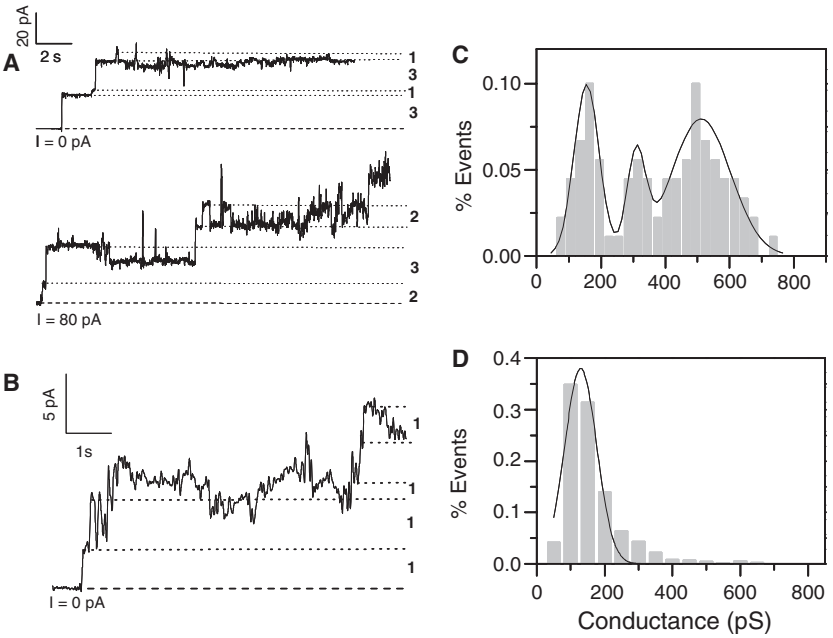

Fig. 4. Pore formation in PLMs by StB-wt and StB-Y31. (A) Ionic current flowing through the membrane increases stepwise after addition of 3–4 μM of the native StB-wt. The protein was added to the *cis* side when a constant voltage of +40 mV was applied. After opening of the first two or three pores, it is possible to observe some rapid closures or flickering of small channels, corresponding to conductance levels 1 and 2. The amplitude of each step was used to calculate the characteristic pore conductance. The traces are representative of four independent experiments. (B) Current flowing through the membrane induced by the addition of 3–5 μM of StB-Y31 in prefibrillar state. The trace is representative of five experiments. (C,D) The conductance of single pores was used to build up histograms showing the percentage of events observed for a given amplitude. The minimum time interval for defining an open state level was 20 ms. The distribution was fitted with three or one Gaussians curves, giving the mean ± SEM conductances, as described in Table 2. The number of events considered was 94 (StB-wt) and 880 (StB-Y31), obtained from four to seven independent experiments. In all experiments, the membrane composition was PC : PS (2 : 1, w/w) and the buffer solution was 100 mM KCl, 10 mM Tris, 1 mM EDTA (pH 8.5).

lipids, causing increases in the current when applying +40 mV (Fig. 4 and Table 2). Pore-like activity was observed a few seconds after the addition of StB-Y31 in the prefibrillar state; however, a typical step-like current increase similar to StB-wt in the native state was not observed (Fig. 4B). We rather observed one

Table 2. Electrophysiological properties of StB-wt and StB-Y31 in PLM. NA, not active; ND, not determined.

Protein	Salt	Conductance[a] (pS)			(I^+/I^-)[b]	(P^+/P^-)[c]
		Level 1	Level 2	Level 3		
Native StB-wt	NaCl	146 ± 40	292 ± 53	453 ± 22	1.59 ± 0.28	3.9 ± 0.8
Native StB-wt	KCl	155 ± 39	332 ± 29	512 ± 95	1.79 ± 0.13	3.7 ± 0.5
Prefibrillar StB-wt		NA	NA	NA	NA	NA
Native StB-Y31	KCl	124 ± 42			ND	ND
Prefibrillar StB-Y31	KCl	129 ± 47			0.91 ± 0.06	0.30 ± 0.05

[a] Single channel conductance at +40 mV. Values are obtained from the histograms reported in Fig. 4C,D. [b] Ratio between the ion current flowing through the pores when applying +100 mV and −100 mV, as shown in Fig. 5A. Values are the mean ± SEM of three or four experiments. [c] Selectivity expressed as cation/anion permeability ratio was determined as described in the Experimental procedures with 5.5 *trans : cis* gradient. Values are obtained as described in Fig. 5 and are the mean ± SEM of two or three independent experiments.

small conductance state (G = 129 ± 47 pS), similar to the wild-type lower level conductance. Besides these small conductance state pores, which represents the main population with StB-Y31, a minor amount of high conductance state similar to wild-type stefin B could also be observed (Fig. 4D). Native StB-Y31 was less active, but of similar behaviour (Table 2).

The wild-type stefin B current-voltage characteristic was studied in NaCl and KCl solutions, showing asymmetrical behaviour in both cases, with a higher current when a positive voltage was applied (Fig. 5A and Table 2). This nonlinearity is normally related to an asymmetrical distribution of charged amino acids along the lumen of the pore. The wild-type stefin B pores are cation selective (Fig. 5B), with similar reversal potentials (V_{rev}) for Na^+ and K^+ (Table 2). By contrast, StB-Y31 pores were slightly anion selective (Fig. 5B and Table 2). Moreover, pores of StB-Y31 showed voltage-dependent gating (Fig. 6). They opened when high positive voltages were applied (e.g. +120 mV; Fig. 6) and rapidly closed when negative voltages (−120 mV, −100 mV and −80 mV; Fig. 6) were applied. Pores of StB-wt were not affected by the potential (not shown).

G4R mutant in the native and prefibrillar state caused an increase of current when either positive or negative high voltages were applied (> 100 mV) but no stepwise insertions of stable pores were recorded (Fig. 7). Very fast and stochastic membrane perturbing events were observed. Usually, these events lasted milliseconds (sometimes seconds) and their frequency is increased by increasing the voltage applied. Clearly, the activity or interaction of G4R with PLM was not a dose-dependent process. This behaviour is not suprising for amyloid proteins because it has been proposed that only annular structures of prefibrillar amyloid proteins are able to form pores [19]. After G4R addition and increased membrane permeability, the membrane usually broke after some minutes (Fig. 7). This

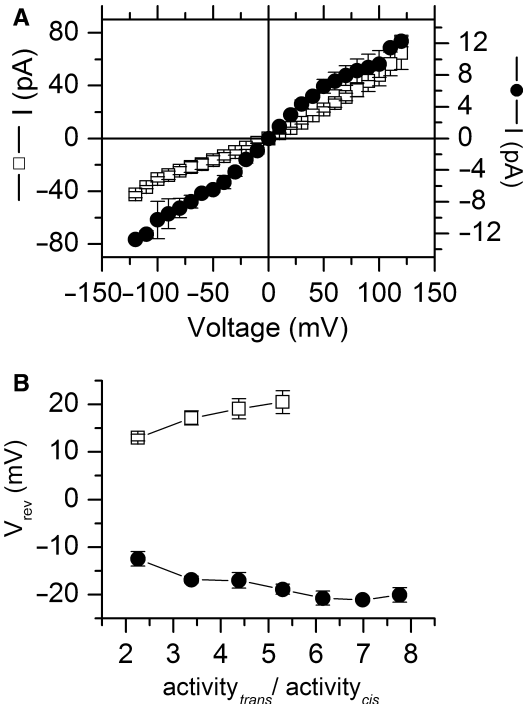

Fig. 5. Dependence of current on applied voltage and selectivity of StB-wt and StB-Y31. (A) The single channel instantaneous I–V characteristic of stefin B variants in 100 mM KCl. The I–V curve was derived from the amplitude of the current steps elicited by square voltage pulses experiments with more than five pores inserted into the membrane. The total current values of three or four independent experiments were normalized for the number of inserted pores. (B) Selectivity of stefin B variants pores. The proteins were added to the *cis* side of a membrane initially bathed with symmetrical 100 mM KCl buffer. The *trans* side solution was increased stepwise with KCl 3 M, after insertion of pores. For each salt concentration, the potential necessary to zero the transmembrane potential (V_{rev}) was reported versus activity$_{trans}$/activity$_{cis}$ (the activities of KCl in *trans* and *cis* side, respectively). Positive V_{rev} means cationic selectivity. Values are the mean ± SEM of three or four independent experiments. □, StB-wt; ●, StB-Y31. Protein concentrations and membrane composition are as described in Fig. 4.

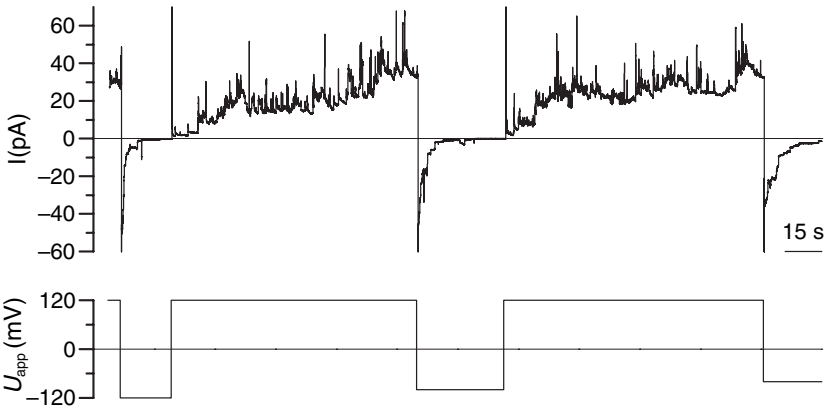

Fig. 6. The closure of StB-Y31 pores is voltage dependent. Current through pores formed by the StB-Y31 isoform is shown when applying a positive (+120 mV) and negative voltage (−120, −100 and −80 mV). The traces are representative of three independent experiments.

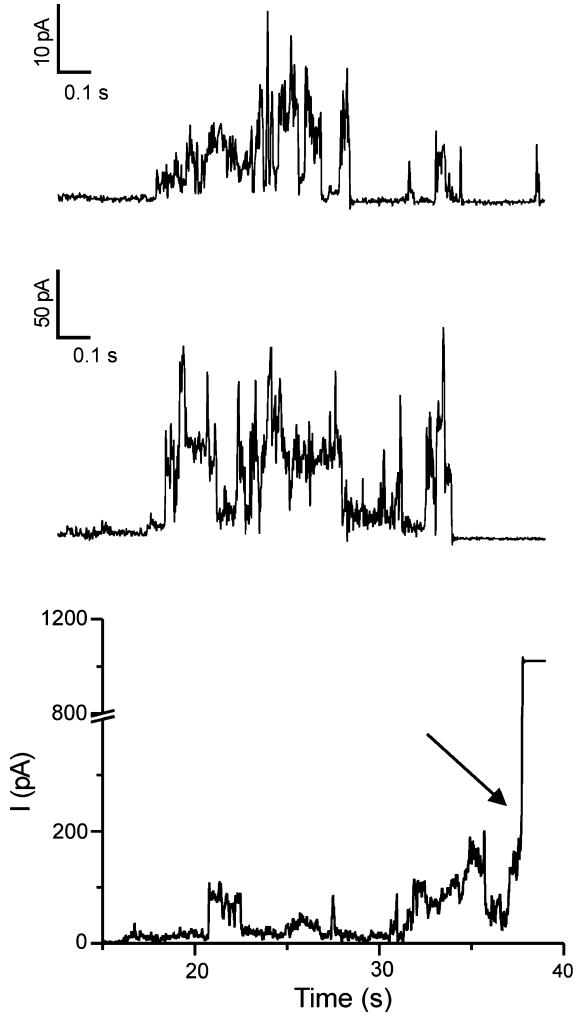

Fig. 7. Membrane destabilization of G4R. The ionic current flowing through the membrane upon addition of 3–4 μM of native G4R. Similar results were obtained with the prefibrillar form of G4R. The traces were acquired at +100 mV. The lower pannel shows a tipical membrane break observed by G4R, which prevented any further electrophysiological characterization. The break is denoted by an arrow. The traces are representative of eight independent experiments.

suggests a strong interaction with the membrane in accordance with the SPR, liposomes and monolayers results.

It has been shown previously that stefin A does not form amyloid fibrils at conditions used in the present study [35,36] and is unable to permeabilize liposomes [11]; thus, it has been used as a good control. The addition of a μM concentration of stefin A to preformed PLM did not cause any increase in membrane permeability. Stefin A was able to transiently destabilize the membrane only when high voltages were applied (> 100 mV), but no stable pores were formed, nor was the membrane broken (data not shown). Such membrane interaction of stefin A is consistent with the poor insertion ability in monolayers as observed by Anderluh *et al.* [11].

Discussion

In its modified form, the 'amyloid cascade hypothesis' of Alzheimer's disease [37] states that a detrimental cascade of events leading to cell dysfunction, and eventually cell death, is due to protofibrillar intermediates of Aβ peptide [38,39]. Soluble Aβ oligomers, which proved toxic to neurons [38], are known under various names: micelles, protofibrils, prefibrillar aggregates and amyloid-derived diffusible ligands [8]. The size and conformation of the most toxic species is under investigation.

Membrane interactions of Aβ oligomers have been extensively studied [20,21]. Some studies even formulated the so called 'channel hypothesis' of Alzheimer's disease [12], which states that amyloidogenic peptides form cation selective channels [13,16,40]. Apart from Aβ, at least six other amyloidogenic peptides were shown to make pores into membranes [17]. Apart from direct perforation, other more specific membrane interactions may take place. For example, gangliosides bind Aβ and change its conformation

to a β-sheet [20]. The present study aimed to characterize the membrane interaction and pore-forming ability of three human stefin B variants in native and prefibrillar states.

The results of all of the biophysical approaches used in the present study may be summarized by two key observations: (a) zwitterionic PC membranes were a poor substrate in any of the tests for native or prefibrillar forms of proteins and (b) the association of prefibrillar G4R with the model lipid systems used was better than for the other two variants. The association of prefibrillar forms of amyloidogenic proteins preferentially with negatively charged lipids might have physiological consequences because negatively charged lipids are mainly found in the membranes within the cell. In our case, the effects of proteins were clearly much more pronounced when negatively charged lipids were used. For example, critical pressures were higher for PG monolayers and were close to 30 $mN{\cdot}m^{-1}$ for G4R, as reported as the surface pressure encountered in biological membranes [41]. Furthermore, the release of calcein only took place from PG liposomes (Fig. 2) and considerable binding occurred only for prefibrillar forms to PG LUV (Fig. 3). An exception was the binding of StB-Y31 to PC liposomes, as revealed by SPR (Fig. 3A), where considerable membrane binding was demonstrated. The tyrosine side-chain may contribute to the better membrane association, in agreement with the observation that aromatic amino acids contribute significantly to the free energy of transfer of model peptides from water to the interphase [42] and are important for the attachment of peripheral proteins to lipid membrane. The SPR result, taken together with the changed ion selectivity of this variant compared to the wild-type (Fig. 5), clearly indicates that this residue is interacting with the membrane and is located within the lumen of the pores once they are formed.

The mutant G4R showed the best association with the model monolayers and bilayers under study. It showed the highest critical pressures in lipid monolayers (Table 1) and bound to the highest level to PG LUV (Fig. 3). It was also much more efficient in perturbing the membrane stability than other two variants, as demonstrated by calcein release experiments (Fig. 2) and the ability to break PLMs (Fig. 7). It is possible that the lipid domain structure could affect interaction of G4R with the model lipid systems used. It was shown that negatively charged lipids may mix non-ideally with phosphatidylcholine [43]. However, because these effects were observed only with G4R, they may be partly explained by an additional positive charge on the mutant and indicate that electrostatic interactions have an important role in the association with a negatively charged membrane. It must not be overlooked from the physiological point of view that this mutant has been found in some EPM1 patients and its aggregation behaviour was predicted to possibly contribute to signs of the disease [29].

The most surprising result is that the native wild-type stefin B is able to incorporate into lipid bilayers containing negatively charged lipids by forming well defined and cation selective pores (Fig. 4A). Compared to the specialized pore-forming toxins, which are active at nano- or picomolar concentrations, a high protein concentration was used in the present study. Nevertheless, the pore-forming process appears to be significant because the same amount of the closely-related stefin A did not show any pore formation or membrane interaction. The low activity of stefin B compared to pore-forming toxins can be understood if only a fraction of the protein (possibly the higher oligomers) was active towards membranes.

High-conductance channels form a few seconds after protein addition to the *cis* side of the bilayer. Moreover, it was possible to identify the presence of fast- and short-lived states characterized by lower conductances. The multiple conductance state has been already shown in other cation selective amyloid peptides [12,16]. StB-wt channel activity is characterized by the presence of pS conductances, whereas no nanosiemens event as for Aβ [12,16], has been identified in the present study. The nonpathological stB-Y31 isoform shows different electrophysiological characteristics. This more amyloidogenic variant is able to form pores with small conductances when in the prefibrilar state. Once inserted into the lipid bilayer, the pores stay open most of the time and display anion selectivity and voltage dependence (Figs 4–6). Interestingly, the pathological mutant G4R is unable to form pores. According to the results obtained by SPR and for monolayers, it is evident that G4R, in the prefibrillar state, strongly interacts with the lipid bilayer causing the membrane break. This effect has been demonstrated at various protein concentrations, suggesting that it is a peculiarity of G4R rather than a concentration effect. It has been suggested that only annular prefibrillar structures are involved in the pore formation processes [19]. Thus, Y31 variant and the wild-type protein could form pores by the same oligomer and/or structural organizations (i.e globular, chain like or annular). In this case, our results suggest that different electrophysiological properties of StB-Y31 are due to the lack of the negative charge (Tyr instead of Glu at position 31), which should lie in the lumen of the pore.

To emphasize once more, the wild-type protein can form cation selective pores already at neutral pH, which may not be deleterious for the cell and could offer the means of a regulatory mechanism. Stefin B was often found to be overexpressed in neurodegenerative conditions, such as amyotrophic lateral sclerosis, Alzheimer's disease and epilepsy. However, no amyloid pathology is known for this protein to date, and its main pathology remains as EPM1 [28]. Alternative functions other than protease inhibition are possible for stefin B. It has been found as part of a multiprotein complex specific to the cerebellum in which none of the partners was a protease [44]. It is possible that the protein could, under certain stressful circumstances for the cell, adopt new functions (i.e. perforate negatively charged membranes). Such a connection was suggested for endostatin [45]. Furthermore, stefin B is involved in the invertebrate innate immunity response [46], which is thought to be a precedent of verterbrate/mammalian innate immunity [47]. A possible physiological role of pores formed by Aβ peptide was also suggested, which could actually improve rather than decrease neuronal viability [48].

It is still not clear whether amyloid membrane pore formation is a process occurring *in vivo*, both in physiological and/or pathological conditions. It may be just an epiphenomenon shared by different amyloid proteins. The results of the present study were obtained with native and prefibrillar states, which are composed of different oligomeric species. Thus, it could be possible that the differences observed between the variants are due to a different distribution of superstructures. In this case, different super-organization may act differently on the model membrane. Nevertheless, some clear conclusions can be drawn. Similar to other amyloid-forming proteins, StB-wt and StB-Y31 exert pore-forming activity and G4R exerts strong membrane interacting effects. At present, we do not know the physiological or pathological relevance of these events, but the results provided here represent further evidence to suggest that prefibrillar aggregates of amyloidogenic proteins share similar pore-like properties.

Experimental procedures

Materials

PC, PG and PS were from Avanti Polar Lipids (Alabaster, AL, USA). All other chemicals were obtained from Sigma (St Louis, MO, USA) unless stated otherwise. The concentration of PC was determined with Free Phospholipids B kit according to the manufacturer's instructions (Wako Chemicals, Dusseldorf, Germany).

Protein isolation

All three stefin B variants were prepared as recombinant proteins as previously described [49,50]. Cysteine at position 3 was changed to Ser to avoid covalent oligomer formation in all proteins [50]. In brief, isolation procedure was as follows: after expression in *Escherichia coli*, cell lysate was purified by affinity chromatography on a CM-papain-Sepharose followed by SEC on Sephacryl S-200. Fractions with inhibitory activity against papain were collected. Affinity chromatography was replaced by another SEC step on Sephacryl S-200 for StB-Y31 and G4R.

Preparing the prefibrillar aggregates

Preparation procedure and the buffer was exactly the same as described previously [30,50]. Briefly, proteins were incubated in 0.015 M acetate buffer (pH 4.8) (0.15 M NaCl) for 5–7 days to yield prefibrillar aggregates. Morphologies of the aggregates, recorded by transmission electron microscopy and atomic force microscopy, have been reported previously [30,31].

Oligomeric state

All three proteins have preserved secondary and tertiary structure, as shown by CD spectroscopy [50]. SEC purified stefin B wild-type and G4R samples at pH 7, where the proteins are native, are composed of monomers, dimers, tetramers and some higher order oligomers, whereas the Y31 stefin B isoform is predominantly dimeric (E. Žerovnik, unpublished observation). The ratio between the oligomers varies with the number of freeze and thaw cycles and is not affected by the pH in the physiological range (i.e. pH 6.5–8) We ensured that the proteins were always prepared the same way; therefore, StB-wt and the G4R samples were composed of approximately 25% monomers, 45% dimers, 20% tetramers and 10% higher order oligomers. The prefibrillar forms, obtained by incubation of the proteins at pH 4.8 for approximately 1 week, are morphologically micelle-like aggregates, whereas the oligomer seen by SDS upon cross-linking is a dimer [31].

Liposome permeabilization assay

Lipid mixtures, dissolved in chloroform, were spread on a round-bottom glass flask of a rotary evaporator and dried under vacuum for at least 3 h. The lipid film was resuspended in 1 mL of vesicle buffer (140 mM NaCl, 20 mM Tris–HCl, pH 8.5, 1 mM EDTA) with or without 60 mM calcein and freeze-thawed six times. The resulting multi-lamellar vesicles were converted to LUV by

extrusion through 100 nm polycarbonate membranes [51]. The excess of calcein was removed from the calcein-loaded liposomes by gel filtration on a small G-50 column. Vesicles were stored at 4 °C immediately after preparation and used within 2 days. For calcein release experiments, liposomes at 30 μM final concentration were mixed with protein in 0.5 mL and incubated overnight at room temperature. Vesicle buffer (0.5 mL) was then added to the samples, which were centrifuged for 10 min at 16 000 ***g*** in a benchtop centrifuge. The supernatant was transferred to another tube and the released calcein measured using a Jasco FP-750 spectrofluorimeter (Jasco Inc., Easton, MD, USA), with excitation and emission at 485 and 520 nm. Excitation and emission slits were set to 5 nm. For the time course measurements, protein was incubated at desired concentrations in a 1 mL cuvette and stirred at 25 °C. Vesicles were added at the required concentration and the time course was followed for 30 min. The permeabilization induced by the proteins was expressed as a percentage of the maximal permeabilization obtained at the end of the assay by the addition of Triton X-100 to a final concentration of 2 mM.

Surface pressure measurements

Surface pressure measurements were carried out with a MicroTrough-S system from Kibron (Helsinki, Finland) at room temperature. The aqueous sub-phase consisted of 500 μL of 10 mM Hepes, 200 mM NaCl (pH 7.5). Lipids dissolved in chloroform/methanol (2 : 1) were gently spread over the sub-phase. Changing the amount of lipid applied to the air–water interface attained the desired initial surface pressure. After approximately 10 min, to allow for solvent evaporation, the desired stefin variant was injected through a hole connected to the sub-phase. The final protein concentration in the Langmuir trough was 10 μM. The increment in surface pressure versus time was recorded until a stable signal was obtained.

SPR

The binding to the supported liposomes was measured by a Biacore X (Biacore). Liposome-covered surface was prepared as described [52]. The L1 chip was equilibrated in vesicle buffer. LUV were injected at 0.5 mM lipid concentration across the chip for 15 min at a flow-rate of 1 $\mu L \cdot min^{-1}$. Loosely bound vesicles were eluted from the chip by three 1 min injections of 100 mM NaOH. Unspecific binding sites were blocked by one 1 min injection of 0.1 $mg \cdot mL^{-1}$ bovine serum albumin. For the binding experiment, proteins were injected at a concentration of 10–70 μM for 120 s at 20 $\mu L \cdot min^{-1}$. Blanks were injections of buffer without protein.

PLM

PLM was made of PC/PS (2 : 1; w/w) with a folded bilayer method [53] and formed across a 180 μm diameter hole on a 25 μm thick Teflon sheet. The protein was added at a micromolar concentration to stable preformed bilayers on the *cis* compartment only, which was filled with 100 mM KCl, 20 mM Tris, 1 mM EDTA (pH 8.5). The potential was applied to the *cis* compartment, with the *trans* one being the reference. All the experiments were started in symmetrical conditions, using the same buffer on both compartments (2 mL each). Channel openings were observed usually at +40 mV applied potential. The current across the bilayer was measured and the conductance (G) was determined as [54]:

$$G\,[\mathrm{pS}] = I\,[\mathrm{pA}]/U\,[\mathrm{V}] \quad (1)$$

where I is the current through the membrane when applying a transmembrane potential, U.

Macroscopic currents were recorded by a patch clamp amplifier (Axopatch 200; Axon Instruments, Foster City, CA, USA). The current traces were low-pass filtered at 0.3 kHz and acquired at 2 kHz on a computer using AXOSCOPE 8 software and DigiData 1200 A/D converter (Axon Instruments). All measurements were performed at room temperature.

For the selectivity measurements, KCl concentration was stepwise increased on the *trans* side using 3 M KCl, 20 mM Tris, 1 mM EDTA (pH 8.5), until an eight-fold concentration gradient was obtained. At each concentration, the potential necessary to zero the transmembrane current [i.e. the reversal voltage (U_{rev})] was determined. From the reversal voltage, the ratio of the cation over anion permeability (P_+/P_-) was calculated using the Goldman–Hodgkin–Katz equation [55]:

$$P_+/P_- = [(a_{trans}/a_{cis}) \times \exp(eU_{rev}/kT) - 1]/[(a_{trans}/a_{cis}) - \exp(eU_{rev}/kT)] \quad (2)$$

where a_{trans} and a_{cis} are the activities of KCl in *trans* and *cis* side, respectively, and kT/*e* is approximately 25 mV at room temperature.

Acknowledgements

We thank Luise Kroon Žitko (JSI, Ljubljana) for help with the stefin B protein purification. This work was funded by grant P1-0140 from the Ministry of Higher Education, Science and Technology of the Republic Slovenia by the Slovenian Research Agency (ARRS).

References

1 Ross CA & Poirier MA (2004) Protein aggregation and neurodegenerative disease. *Nat Med* **10**, S10–S17.

2 Dobson CM (2002) Getting out of shape. *Nature* **418**, 729–730.
3 Almeida CG, Takahashi RH & Gouras GK (2006) Beta-amyloid accumulation impairs multivesicular body sorting by inhibiting the ubiquitin-proteasome system. *J Neurosci* **26**, 4277–4288.
4 Dobson CM (1999) Protein misfolding, evolution and disease. *Trends Biochem Sci* **24**, 329–332.
5 Stefani M & Dobson CM (2003) Protein aggregation and aggregate toxicity: new insights into protein folding, misfolding diseases and biological evolution. *J Mol Med* **81**, 678–699.
6 Baglioni S, Casamenti F, Bucciantini M, Luheshi LM, Taddei N, Chiti F, Dobson CM & Stefani M (2006) Prefibrillar amyloid aggregates could be generic toxins in higher organisms. *J Neurosci* **26**, 8160–8167.
7 Kayed R, Head E, Thompson JL, McIntire TM, Milton SC, Cotman CW & Glabe CG (2003) Common structure of soluble amyloid oligomers implies common mechanism of pathogenesis. *Science* **300**, 486–489.
8 Green JD, Goldsbury C, Kistler J, Cooper GJ & Aebi U (2004) Human amylin oligomer growth and fibril elongation define two distinct phases in amyloid formation. *J Biol Chem* **279**, 12206–12212.
9 Necula M, Kayed R, Milton S & Glabe CG (2007) Small molecule inhibitors of aggregation indicate that amyloid oligomerization and fibrillization pathways are independent and distinct. *J Biol Chem* **282**, 10311–10324.
10 Mirzabekov TA, Lin MC & Kagan BL (1996) Pore formation by the cytotoxic islet amyloid peptide amylin. *J Biol Chem* **271**, 1988–1992.
11 Anderluh G, Gutiérrez-Aguirre I, Rabzelj S, Čeru S, Kopitar-Jerala N, Maček P, Turk V & Žerovnik E (2005) Interaction of human stefin B in the prefibrillar oligomeric form with membranes. Correlation with cellular toxicity. *FEBS J* **272**, 3042–3051.
12 Kagan BL, Hirakura Y, Azimov R, Azimova R & Lin MC (2002) The channel hypothesis of Alzheimer's disease: current status. *Peptides* **23**, 1311–131510.
13 Arispe N, Pollard HB & Rojas E (1993) Giant multilevel cation channels formed by Alzheimer disease amyloid beta-protein [A beta P-(1-40)] in bilayer membranes. *Proc Natl Acad Sci U S A* **90**, 10573–10577.
14 Arispe N, Pollard HB & Rojas E (1994) beta-Amyloid Ca(2+)-channel hypothesis for neuronal death in Alzheimer disease. *Mol Cell Biochem* **140**, 119–125.
15 Kayed R, Sokolov Y, Edmonds B, McIntire TM, Milton SC, Hall JE & Glabe CG (2004) Permeabilization of lipid bilayers is a common conformation-dependent activity of soluble amyloid oligomers in protein misfolding diseases. *J Biol Chem* **279**, 46363–46366.
16 Arispe N, Rojas E & Pollard HB (1993) Alzheimer disease amyloid beta protein forms calcium channels in bilayer membranes: blockade by tromethamine and aluminum. *Proc Natl Acad Sci U S A* **90**, 567–571.
17 Kawahara M, Kuroda Y, Arispe N & Rojas E (2000) Alzheimer's beta-amyloid, human islet amylin, and prion protein fragment evoke intracellular free calcium elevations by a common mechanism in a hypothalamic GnRH neuronal cell line. *J Biol Chem* **275**, 14077–14083.
18 Quist A, Doudevski I, Lin H, Azimova R, Ng D, Frangione B, Kagan B, Ghiso J & Lal R (2005) Amyloid ion channels: a common structural link for protein-misfolding disease. *Proc Natl Acad Sci U S A* **102**, 10427–10432.
19 Lashuel HA & Lansbury PT Jr (2006) Are amyloid diseases caused by protein aggregates that mimic bacterial pore-forming toxins? *Q Rev Biophys* **39**, 167–201.
20 Matsuzaki K (2007) Physicochemical interactions of amyloid β-peptide with lipid bilayers. *Biochim Biophys Acta* **1768**, 1935–1942.
21 Yanagisawa K (2007) Role of gangliosides in Alzheimer's disease. *Biochim Biophys Acta* **1768**, 1943–1951.
22 Turk V, Turk B & Turk D (2001) Lysosomal cysteine proteases: facts and opportunities. *EMBO J* **20**, 4629–4633.
23 Palsdottir A, Abrahamson M, Thorsteinsson L, Arnason A, Olafsson I, Grubb A & Jensson O (1989) Mutation in the cystatin C gene causes hereditary brain hemorrhage. *Prog Clin Biol Res* **317**, 241–246.
24 Cathcart HM, Huang R, Lanham IS, Corder EH & Poduslo SE (2005) Cystatin C as a risk factor for Alzheimer disease. *Neurology* **64**, 755–757.
25 Maruyama K, Kametani F, Ikeda S, Ishihara T & Yanagisawa N (1992) Characterization of amyloid fibril protein from a case of cerebral amyloid angiopathy showing immunohistochemical reactivity for both beta protein and cystatin C. *Neurosci Lett* **144**, 38–42.
26 Sastre M, Calero M, Pawlik M, Mathews PM, Kumar A, Danilov V, Schmidt SD, Nixon RA, Frangione B & Levy E (2004) Binding of cystatin C to Alzheimer's amyloid beta inhibits *in vitro* amyloid fibril formation. *Neurobiol Aging* **25**, 1033–1043.
27 Ii K, Ito H, Kominami E & Hirano A (1993) Abnormal distribution of cathepsin proteinases and endogenous inhibitors (cystatins) in the hippocampus of patients with Alzheimer's disease, parkinsonism-dementia complex on Guam, and senile dementia and in the aged. *Virchows Arch A Pathol Anat Histopathol* **423**, 185–194.
28 Pennacchio LA, Lehesjoki AE, Stone NE, Willour VL, Virtaneva K, Miao J, D'Amato E, Ramirez L, Faham M, Koskiniemi M *et al.* (1996) Mutations in the gene encoding cystatin B in progressive myoclonus epilepsy (EPM1). *Science* **271**, 1731–1734.
29 Čeru S, Rabzelj S, Kopitar-Jerala N, Turk V & Žerovnik E (2005) Protein aggregation as a possible cause for

pathology in a subset of familial Unverricht-Lundborg disease. *Med Hypotheses* **64**, 955–959.
30 Žerovnik E, Pompe-Novak M, Škarabot M, Ravnikar M, Muševič I & Turk V (2002) Human stefin B readily forms amyloid fibrils *in vitro*. *Biochim Biophys Acta* **1594**, 1–5.
31 Žerovnik E, Škarabot M, Škerget K, Giannini S, Stoka V, Jenko-Kokalj S & Staniforth RA (2007) Amyloid fibril formation by human stefin B: influence of pH and TFE on fibril growth and morphology. *Amyloid* **14**, 237–247.
32 Gorbenko GP & Kinnunen PK (2006) The role of lipid-protein interactions in amyloid-type protein fibril formation. *Chem Phys Lipids* **141**, 72–82.
33 Hirakura Y, Lin MC & Kagan BL (1999) Alzheimer amyloid abeta1-42 channels: effects of solvent, pH, and Congo Red. *J Neurosci Res* **57**, 458–466.
34 Sokolov Y, Kozak JA, Kayed R, Chanturiya A, Glabe C & Hall JE (2006) Soluble amyloid oligomers increase bilayer conductance by altering dielectric structure. *J Gen Physiol* **128**, 637–647.
35 Jenko S, Škarabot M, Kenig M, Gunčar G, Muševič I, Turk D & Žerovnik E (2004) Different propensity to form amyloid fibrils by two homologous proteins-Human stefins A and B: searching for an explanation. *Proteins* **55**, 417–425.
36 Žerovnik E (2002) Amyloid-fibril formation. Proposed mechanisms and relevance to conformational disease. *Eur J Biochem* **269**, 3362–3371.
37 Hardy JA & Higgins GA (1992) Alzheimer's disease: the amyloid cascade hypothesis. *Science* **256**, 184–185.
38 Hartley DM, Walsh DM, Ye CP, Diehl T, Vasquez S, Vassilev PM, Teplow DB & Selkoe DJ (1999) Protofibrillar intermediates of amyloid beta-protein induce acute electrophysiological changes and progressive neurotoxicity in cortical neurons. *J Neurosci* **19**, 8876–8884.
39 Walsh DM, Hartley DM, Kusumoto Y, Fezoui Y, Condron MM, Lomakin A, Benedek GB, Selkoe DJ & Teplow DB (1999) Amyloid beta-protein fibrillogenesis. Structure and biological activity of protofibrillar intermediates. *J Biol Chem* **274**, 25945–25952.
40 Arispe N, Pollard HB & Rojas E (1996) Zn2+ interaction with Alzheimer amyloid beta protein calcium channels. *Proc Natl Acad Sci U S A* **93**, 1710–1715.
41 Marsh D (1996) Lateral pressure in membranes. *Biochim Biophys Acta Rev Biomembr* **1286**, 183–223.
42 Wimley WC & White SH (1996) Experimentally determined hydrophobicity scale for proteins at membrane surfaces. *Nature Struct Biol* **3**, 842–848.
43 Huang JW, Swanson JE, Dibble ARG, Hinderliter AK & Feigenson GW (1993) Nonideal mixing of phosphatidylserine and phosphatidylcholine in the fluid lamellar phase. *Biophys J* **64**, 413–425.
44 Di Giaimo R, Riccio M, Santi S, Galeotti C, Ambrosetti DC & Melli M (2002) New insights into the molecular basis of progressive myoclonus epilepsy: a multiprotein complex with cystatin B. *Hum Mol Genet* **11**, 2941–2950.
45 Zhao H, Jutila A, Nurminen T, Wickstrom SA, Keski-Oja J & Kinnunen PK (2005) Binding of endostatin to phosphatidylserine-containing membranes and formation of amyloid-like fibers. *Biochemistry* **44**, 2857–2863.
46 Lefebvre C, Cocquerelle C, Vandenbulcke F, Hot D, Huot L, Lemoine Y & Salzet M (2004) Transcriptomic analysis in the leech Theromyzon tessulatum: involvement of cystatin B in innate immunity. *Biochem J* **380**, 617–625.
47 Salzet M, Tasiemski A & Cooper E (2006) Innate immunity in lophotrochozoans: the annelids. *Curr Pharm Des* **12**, 3043–3050.
48 Plant LD, Boyle JP, Smith IF, Peers C & Pearson HA (2003) The production of amyloid beta peptide is a critical requirement for the viability of central neurons. *J Neurosci* **23**, 5531–5535.
49 Jerala R, Trstenjak M, Lenarčič B & Turk V (1988) Cloning a synthetic gene for human stefin B and its expression in *E. coli*. *FEBS Lett* **239**, 41–44.
50 Rabzelj S, Turk V & Žerovnik E (2005) In vitro study of stability and amyloid-fibril formation of two mutants of human stefin B (cystatin B) occurring in patients with EPM1. *Protein Sci* **14**, 2713–2722.
51 MacDonald RC, MacDonald RI, Menco BP, Takeshita K, Subbarao NK & Hu L (1991) Small-volume extrusion apparatus for preparation of large unilamellar vesicles. *Biochim Biophys Acta* **1061**, 297–303.
52 Anderluh G, Beseničar M, Kladnik A, Lakey JH & Maček P (2005) Properties of nonfused liposomes immobilized on an L1 Biacore chip and their permeabilization by a eukaryotic pore-forming toxin. *Anal Biochem* **344**, 43–52.
53 Dalla Serra M & Menestrina G (2000) Characterization of molecular properties of pore-forming toxins with planar lipid bilayers. *Methods Mol Biol* **145**, 171–188.
54 Menestrina G (1991) Electrophysiological Methods for the Study of Toxin-Membrane Interaction. In *Sourcebook of Bacterial Protein Toxins* (Alouf JE & Freer JH, eds), pp. 215–242. Academic Press, London.
55 Hille B (1984) *Ionic Channels of Excitable Membranes*. Sinauer Associate Publishers, Sunderland, MA.